

# Human respiratory muscle actions and control during exercise

A. ALIVERTI,<sup>1</sup> S. J. CALA,<sup>2</sup> R. DURANTI,<sup>4</sup> G. FERRIGNO,<sup>1</sup> C. M. KENYON,<sup>2</sup>  
A. PEDOTTI,<sup>1</sup> G. SCANO,<sup>4</sup> P. SLIWINSKI,<sup>2</sup> PETER T. MACKLEM,<sup>2</sup> AND S. YAN<sup>3</sup>

<sup>1</sup>Politecnico di Milano, Dipartimento di Bioingegneria, Centro di Bioingegneria, Milan, Italy; <sup>2</sup>Meakins-Christie Laboratories, McGill University, and <sup>3</sup>Montréal Chest Institute, Montreal, Quebec, Canada H2X 2P4; and <sup>4</sup>First Clinica Medica III, Università di Firenze, Florence, Italy

**Aliverti, A., S. J. Cala, R. Duranti, G. Ferrigno, C. M. Kenyon, A. Pedotti, G. Scano, P. Sliwinski, Peter T. Macklem, and S. Yan.** Human respiratory muscle actions and control during exercise. *J. Appl. Physiol.* 83(4): 1256–1269, 1997.—We measured pressures and power of diaphragm, rib cage, and abdominal muscles during quiet breathing (QB) and exercise at 0, 30, 50, and 70% maximum workload ( $\dot{W}_{max}$ ) in five men. By three-dimensional tracking of 86 chest wall markers, we calculated the volumes of lung- and diaphragm-apposed rib cage compartments ( $V_{rc,p}$  and  $V_{rc,a}$ , respectively) and the abdomen ( $V_{ab}$ ). End-inspiratory lung volume increased with percentage of  $\dot{W}_{max}$  as a result of an increase in  $V_{rc,p}$  and  $V_{rc,a}$ . End-expiratory lung volume decreased as a result of a decrease in  $V_{ab}$ .  $\Delta V_{rc,a}/\Delta V_{ab}$  was constant and independent of  $\dot{W}_{max}$ . Thus we used  $\Delta V_{ab}/time$  as an index of diaphragm velocity of shortening. From QB to 70%  $\dot{W}_{max}$ , diaphragmatic pressure ( $P_{di}$ ) increased ~2-fold, diaphragm velocity of shortening 6.5-fold, and diaphragm workload 13-fold. Abdominal muscle pressure was ~0 during QB but was equal to and 180° out of phase with rib cage muscle pressure at all percent  $\dot{W}_{max}$ . Rib cage muscle pressure and abdominal muscle pressure were greater than  $P_{di}$ , but the ratios of these pressures were constant. There was a gradual inspiratory relaxation of abdominal muscles, causing abdominal pressure to fall, which minimized  $P_{di}$  and decreased the expiratory action of the abdominal muscles on  $V_{rc,a}$  gradually, minimizing rib cage distortions. We conclude that from QB to 0%  $\dot{W}_{max}$  there is a switch in respiratory muscle control, with immediate recruitment of rib cage and abdominal muscles. Thereafter, a simple mechanism that increases drive equally to all three muscle groups, with drive to abdominal and rib cage muscles 180° out of phase, allows the diaphragm to contract quasi-isotonically and act as a flow generator, while rib cage and abdominal muscles develop the pressures to displace the rib cage and abdomen, respectively. This acts to equalize the pressures acting on both rib cage compartments, minimizing rib cage distortion.

rib cage distortion; velocity of shortening; respiratory kinematics; flow generation; diaphragm; power

THE RESPIRATORY MUSCLES, like all skeletal muscles, shorten at a particular velocity and develop force. Respiratory muscle shortening is usually measured as the change in volume of a structure that the muscle displaces (rib cage, abdomen, or lungs); velocity of shortening can be measured as flow and force as pressure. From these variables, one can calculate work and power.

Noninvasive estimates of shortening and velocity require accurate measurement of chest wall kinematics. Most of the available information on chest wall

kinematics is based on the two-compartment chest wall model of Konno and Mead (21) composed of rib cage and abdomen, each behaving with a single degree of freedom, so that changes in volume of each compartment<sup>1</sup> can be measured by a single dimension. This may not be sufficient during exercise, when the limits established by Konno and Mead for behavior with two degrees of freedom are exceeded. Indeed, it has been shown that the chest wall moves with more than two degrees of freedom during exercise (2, 15, 16) and even during breathing at rest (30).

The two-compartment rib cage model developed by Ward et al. (30) may be more appropriate for the study of chest wall kinematics in exercise. This model takes into consideration the fact that the lung- and diaphragm-apposed parts of the rib cage ( $RC_p$  and  $RC_a$ , respectively) are exposed to substantially different pressures on their inner surface during inspiration (1), that the diaphragm acts directly only on  $RC_a$ , and that nondiaphragmatic inspiratory muscles act largely on  $RC_p$ .

Displacement of  $RC_p$  is the net result of the action of nondiaphragmatic inspiratory muscles, expiratory rib cage muscles, pleural pressure ( $P_{pl}$ ) over the surface of the lung, and rib cage distortions between  $RC_p$  and  $RC_a$ , which apply a restoring force ( $P_{link}$ ) to  $RC_p$  (8, 20, 30).  $RC_a$  is displaced by the diaphragm, the abdominal muscles (11, 24), and  $P_{pl}$  in the area of apposition of diaphragm to rib cage [which can be approximated by abdominal pressure ( $P_{ab}$ )], and the mechanical linkage between  $RC_p$  and  $RC_a$ . The volume of  $RC_a$  ( $V_{rc,a}$ ) and abdominal volume ( $V_{ab}$ ) are important determinants of diaphragmatic fiber length ( $L_{di}$ ); the volume of  $RC_p$  ( $V_{rc,p}$ ) does not influence  $L_{di}$ , except to the extent that it changes  $V_{rc,a}$  via the mechanical linkage between the two rib cage compartments.

We measure the kinematics of the abdomen,  $RC_p$ , and  $RC_a$ , with a three-dimensional optical reflectance motion analysis (ELITE) system described in detail previously (5). We combine these kinematic measurements with simultaneous measurements of  $P_{pl}$  and  $P_{ab}$  to calculate the pressures generated by different respiratory muscle groups during exercise. The dia-

<sup>1</sup> We use the term “abdominal volume” loosely. The abdomen-diaphragm forms a compartment of constant volume, which is the sum of the volume of contents contained within/under the diaphragm and that contained elsewhere in the peritoneal cavity. It is the latter volume to which we refer when we use the term abdominal volume. Any change in this volume requires an equal and opposite change in the volume contained by the diaphragm.

phragm's contribution was measured directly by trans-diaphragmatic pressure ( $P_{di} = P_{ab} - P_{pl}$ ) (3); the pressure work and power developed by other respiratory muscles were measured by departures of dynamic pressure-volume loops from relaxation curves (6, 25, 26).

This approach to the assessment of respiratory muscle activity has been used extensively (6, 25, 26) to measure net inspiratory and expiratory muscle activity. Konno and Mead (22) applied this methodology to the abdomen and thereby measured the pressures developed by the abdominal muscles ( $P_{abm}$ ). Similarly, the pressures developed by inspiratory and expiratory rib cage muscles ( $P_{rcm,i}$  and  $P_{rcm,e}$ , respectively) can be estimated as the difference between the dynamic  $P_{pl}$ - $V_{rc,p}$  loop and the relaxation pressure-volume curve of  $RC_p$  corrected for the pressure resulting when  $RC_p$  and  $RC_a$  are distorted away from their relaxation configuration (8, 20, 30). Integrating the area under the curves of these pressure-volume diagrams gives the work and power of various muscle groups. Because the pressure is known, power can be partitioned into the relative contributions of force and velocity of shortening. We show that the diaphragm acts primarily as a flow generator, while rib cage muscles provide the pressures to displace  $RC_p$  and increase end-inspiratory lung volume. The abdominal muscles provide the pressures to displace the abdomen and decrease end-expiratory lung volume, while the gradual relaxation during inspiration simultaneously acts to prevent rib cage distortion and minimize  $P_{di}$ .

## METHODS

In this study the chest wall was modeled as being composed of  $RC_p$ ,  $RC_a$ , and the abdomen (30).  $\Delta V_{ab}$  was defined as the volume swept by the abdominal wall, as described by Konno and Mead (21). The boundary between  $RC_p$  and  $RC_a$  was assumed to be at the level of the xiphoid. The boundary

between  $RC_a$  and the abdomen was along the lower costal margin anteriorly and at the level of the lowest point of the lower costal margin posteriorly. Chest wall volume ( $V_{cw}$ ) is the sum of  $V_{rc,p}$ ,  $V_{rc,a}$ , and  $V_{ab}$ . End-expiratory and end-inspiratory volume of each compartment was measured at the beginning and the end of inspiratory flow (zero-flow points) relative to that during quiet breathing. The difference between the end-inspiratory and end-expiratory volume of each compartment was calculated as the tidal volume ( $V_T$ ) contribution by each compartment.

The subjects, procedures, protocol, and reliability of the ELITE system to measure  $V_{cw}$  changes during exercise have been detailed elsewhere (20). Briefly, we studied five normal men during 1) quiet breathing at rest, 2) relaxation at different lung volumes, 3) bilateral transcutaneous supramaximal phrenic nerve stimulation at functional residual capacity (FRC) with glottis closed, and 4) during exercise at 0, 30, 50, and 70% of maximum workload ( $\dot{W}_{max}$ ). Exercise at each percent  $\dot{W}_{max}$  was maintained for 3 min and 20 s. Data were acquired during the last 20-s period, when changes in lung volume ( $V_L$ ) were measured by rebreathing from a water-filled spirometer equipped with a  $CO_2$  absorber. Esophageal ( $P_{es}$ ) and gastric ( $P_{ga}$ ) pressures were measured with standard balloon-catheter transducer systems and were used as indexes of  $P_{pl}$  and  $P_{ab}$ .  $P_{di}$  was calculated as  $P_{ga} - P_{es}$ . Active  $P_{di}$  was taken as  $P_{di}$  at end inspiration relative to its end-expiratory baseline during quiet breathing, when  $P_{di}$  was assumed to be zero.  $P_{rcm}$  was measured as the difference between the dynamic  $P_{es}$ - $V_{rc,p}$  loops and the relaxation pressure-volume curve of  $RC_p$ , with the restoring force resulting from rib cage distortion taken into account (30).  $P_{abm}$  was measured as the difference between the dynamic  $P_{ga}$ - $V_{ab}$  loops and the relaxation pressure-volume curve of the abdomen (22). The graphical methods for measuring  $P_{rcm}$  and  $P_{abm}$  are shown in Fig. 1.

Work was measured by the area contained within the pressure-volume loops and power by dividing the work by time. Values are means  $\pm$  SE. Repeated-measures analysis of variance and Dunnett's test were performed to compare each

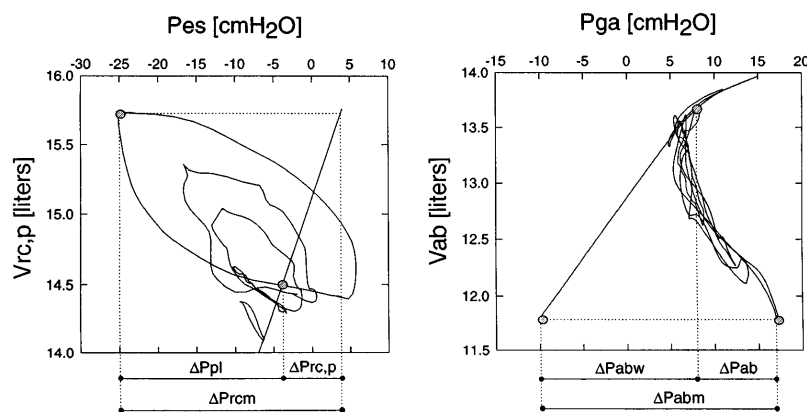


Fig. 1. *Left*: relationship between esophageal pressure ( $P_{es}$ ) as an index of pleural pressure ( $P_{pl}$ ) and volume of pulmonary rib cage ( $V_{rc,p}$ ) during quiet breathing and exercise at 0, 30, 50, and 70% of maximum workload ( $\dot{W}_{max}$ ). Solid straight line, relaxation pressure-volume curve of pulmonary rib cage, which gives elastic recoil pressure of pulmonary rib cage ( $P_{rc,p}$ ) at any  $V_{rc,p}$ . Measurement of pressure generated by rib cage muscles ( $P_{rcm}$ ) at any  $V_{rc,p}$  is obtained from horizontal distance between dynamic loop and relaxation line at that volume corrected for any restoring force resulting from rib cage distortion (20, 30). Points at *left* of relaxation line are inspiratory; those at *right* are expiratory. *Right*: relationship between gastric pressure ( $P_{ga}$ ), used as an index of abdominal pressure ( $P_{ab}$ ), and volume of abdomen ( $V_{ab}$ ) during quiet breathing and at various levels of exercise. Solid straight line, relaxation pressure-volume curve of abdomen, which gives its elastic recoil pressure ( $P_{abw}$ ) at any  $V_{ab}$  below functional residual capacity. Measurement of pressure generated by abdominal muscles ( $P_{abm}$ ) at any  $V_{ab}$  during exercise is obtained from horizontal distance between dynamic loop and relaxation line at that volume.

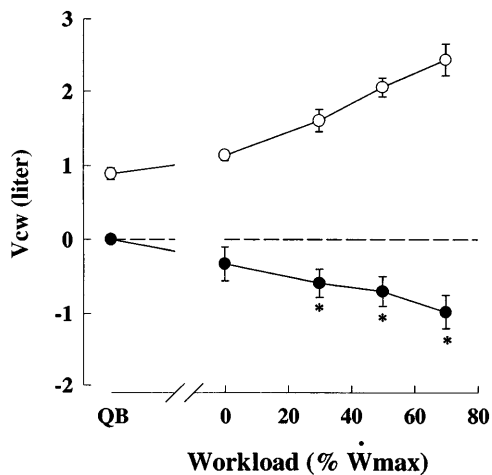


Fig. 2. Chest wall volume ( $V_{cw}$ ) change during exercise. Difference between end-inspiratory ( $\circ$ ) and end-expiratory  $V_{cw}$  ( $\bullet$ ) is tidal volume. Dashed line, end-expiratory  $V_{cw}$  during quiet breathing (QB), which was set to zero. \*Significantly different from end-expiratory volume during quiet breathing.

set of data obtained during quiet breathing and exercise.  $P < 0.05$  was considered as indicating statistical significance.

## RESULTS

### Kinematics

Figure 2 shows end-inspiratory and end-expiratory  $V_{cw}$  during exercise. The vertical distance between the end-inspiratory and end-expiratory points for a given exercise load is the  $V_T$ . There was a progressive decrease in end-expiratory and an increase in end-inspiratory  $V_{cw}$  during exercise ( $P < 0.002$ ). The intersubject variability was large. At 70%  $\dot{W}_{max}$ , the changes in end-expiratory  $V_{cw}$  ranged from  $-0.38$  to  $-1.71$  liters; it averaged  $-0.98$  liter for the group.

With increasing workload, the decrease in end-expiratory  $V_{cw}$  during exercise was almost entirely attributable to the decrease in end-expiratory  $V_{ab}$  ( $P < 0.001$ ; Fig. 3). End-expiratory  $V_{rc,p}$  was constant in three subjects, increased slightly (0.23 liter) in one subject, and decreased moderately (0.48 liter) in one subject at the highest workload. The group mean change in end-expiratory  $V_{rc,p}$  ( $-0.1$  liter at 70%  $\dot{W}_{max}$ ) was not statistically significant ( $P = 0.65$ ). End-expiratory  $V_{rc,a}$  was constant in all subjects ( $P = 0.82$ ). Despite the progressive increase in end-inspiratory  $V_{rc,p}$  and  $V_{rc,a}$ , end-inspiratory  $V_{ab}$  did not in-

crease significantly ( $P = 0.09$ ) with increasing workload.

Because  $L_{di}$  is determined by abdominal and lower rib cage displacements (23), we plotted end-expiratory and end-inspiratory  $V_{rc,a}$  against end-expiratory and end-inspiratory  $V_{ab}$  to assess the relationship between  $V_{rc,a}$  and  $V_{ab}$  during exercise (Fig. 4A). Figure 4A shows that at the beginning of inspiration the relationship shifted horizontally to smaller  $V_{ab}$  at constant  $V_{rc,a}$ , whereas at end inspiration it shifted vertically to greater  $V_{rc,a}$  at nearly constant  $V_{ab}$ . These shifts increased with increasing intensity of exercise. The slope,  $\Delta V_{rc,a}/\Delta V_{ab}$ , did not change significantly from quiet breathing at any level of exercise ( $P = 0.205$ ; Fig. 4B).

### Pressures

*Pressures developed by rib cage muscles.* Figure 5 shows  $V_{rc,p}$ -Pes diagrams of the different subjects during the different levels of exercise. The slopes and intercepts of the RCp relaxation line are given in Table 1. Inspiratory rib cage muscles displace the dynamic loops to the left of the relaxation line; expiratory rib cage muscles displace the dynamic loops to the right. Because the dynamic  $V_{rc,p}$ -Pes trace departs from its relaxation line more and more with the increasing exercise, the nondiaphragmatic inspiratory and expiratory rib cage muscles were progressively recruited as exercise level increased. During an inspiration, the curves show that  $P_{rcm}$  increased monotonically during inspiration, reaching its maximum near end inspiration. Expiratory muscle recruitment caused the dynamic loops to cross the relaxation line. This occurred in four subjects, mostly at heavy exercise. One subject (SY) did not recruit these muscles during exercise, except at the highest level. During quiet breathing there was postinspiratory activity of the inspiratory rib cage muscles throughout expiration; the dynamic  $V_{rc,p}$ -Ppl loop returned to the relaxation line only at end expiration. Even at the highest workload, there was considerable postinspiratory activity of inspiratory rib cage muscles. Expiratory rib cage muscles relaxed rapidly during inspiration.

As shown previously (20), mean rib cage distortion was  $<0.5\%$  at every level of exercise, resulting in mean  $P_{link} < 2.5$  cmH<sub>2</sub>O, usually acting in a direction to make RCp smaller. Thus the correction of the horizontal distance between the dynamic Pes- $V_{rc,p}$  curve to ob-

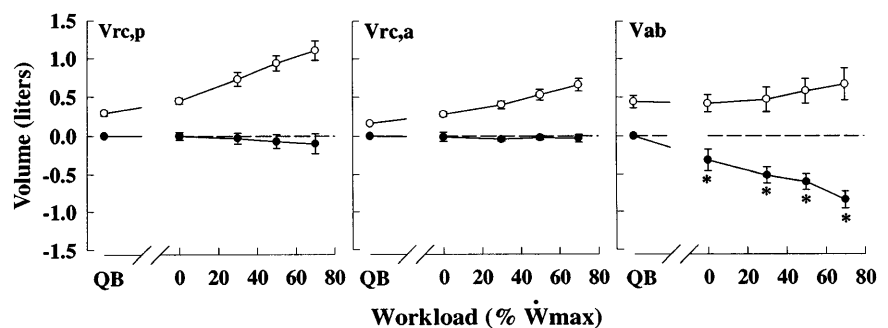


Fig. 3. Changes in  $V_{rc,p}$ , abdominal rib cage volume ( $V_{rc,a}$ ), and  $V_{ab}$  during exercise. Symbols as in Fig. 2.

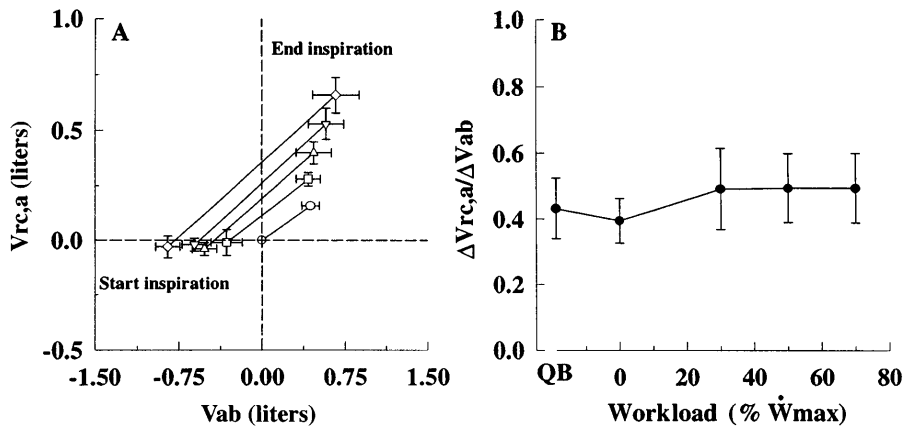


Fig. 4. A: Vrc,a vs. Vab at start and end inspiration. Horizontal and vertical dashed lines correspond to end-expiratory Vrc,a and Vab during quiet breathing, which are designated zero.  $\circ$ , Quiet breathing;  $\square$ , exercise at 0%  $\dot{W}_{max}$ ;  $\triangle$ , exercise at 30%  $\dot{W}_{max}$ ;  $\nabla$ , exercise at 50%  $\dot{W}_{max}$ ;  $\diamond$ , exercise at 70%  $\dot{W}_{max}$ . B: ratio of tidal Vrc,a swing ( $\Delta Vrc,a$ ) to tidal Vab swing ( $\Delta Vab$ ) during exercise. Bars, SD.

tain Prcm was small and essentially constant throughout the breath at all levels of exercise.

**Pressures developed by abdominal muscles.** Figure 6 shows abdominal pressure-volume curves in four of the five subjects. The fifth subject (PG) is not shown, because we could not obtain satisfactory abdominal relaxation curves. Because dynamic pressure curves deviated to the right of the relaxation curve, abdominal expiratory muscles were recruited, even at 0%  $\dot{W}_{max}$ . In striking contrast to the Pes-Vrc,p curves, the dynamic Pga-Vab curves tended to be lines rather than loops. Thus the abdominal muscles gradually relaxed throughout inspiration and fully relaxed only at end inspiration. This resulted in a progressive fall in Pab throughout inspiration, even at 0%  $\dot{W}_{max}$ , in contrast

to the normal inspiratory rise in Pab during quiet breathing. This change in pattern of Pab due to abdominal muscle recruitment has important implications for rib cage dynamics and diaphragm function during exercise.

**Active pressure developed by the diaphragm.** Active Pdi (Fig. 7) was measured at end inspiration relative to the zero Pdi baseline during expiration during quiet breathing. In all but one subject, Pdi fell from quiet breathing to 0%  $\dot{W}_{max}$  and only doubled from quiet breathing to 70%  $\dot{W}_{max}$ .

**Comparison of active pressures developed by the different respiratory muscle groups.** Figure 7 shows the mean values of peak pressures developed by the inspiratory rib cage muscles, the expiratory rib cage muscles,

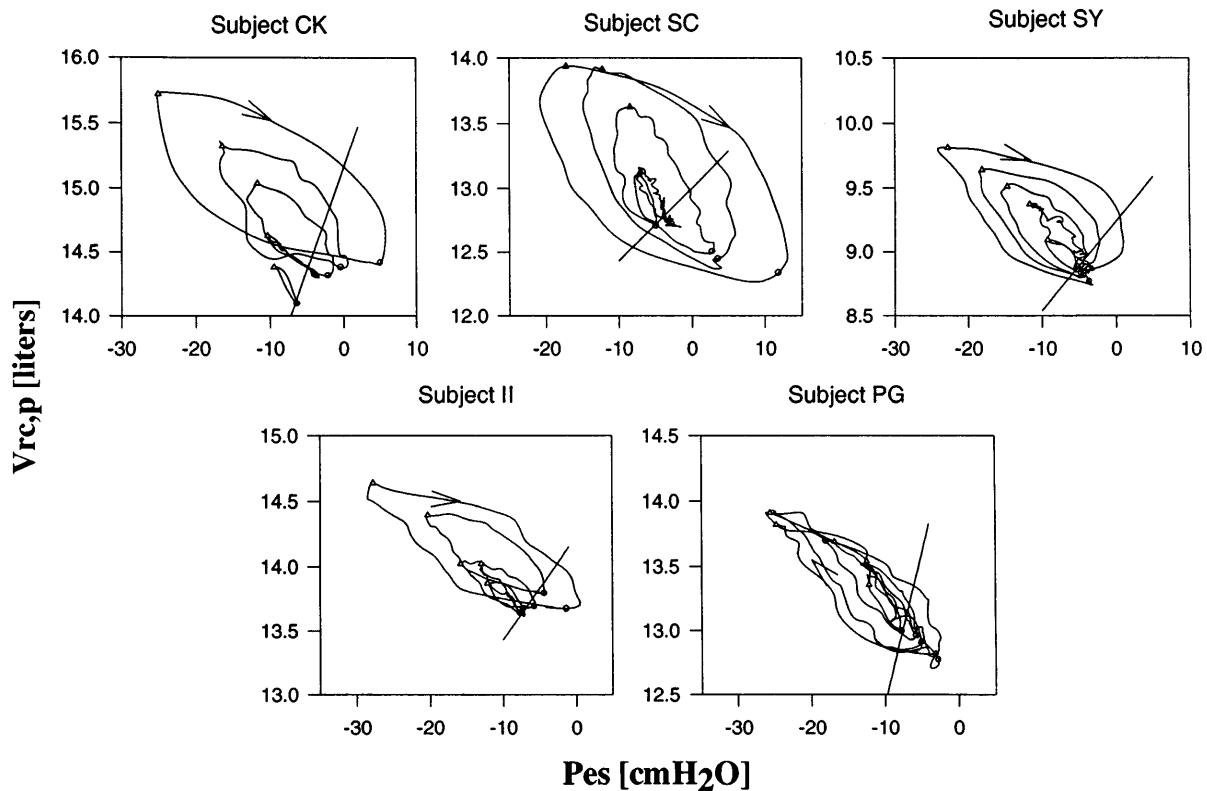


Fig. 5. Vrc,p-Pes loops during quiet breathing and increasing levels of exercise (0, 30, 50, and 70%  $\dot{W}_{max}$ ) and rib cage relaxation lines for all subjects.  $\circ$  and  $\triangle$ , Zero-flow points for end expiration and end inspiration, respectively.



Table 1. Slopes and intercepts of the  $V_{rc,p}$ - $P_{es}$  relaxation lines

Subject	$a$ , l/cmH <sub>2</sub> O	$b$ , liters
CK	0.16	15.13
SC	0.06	12.91
SY	0.07	9.24
II	0.08	14.23
PG	0.23	14.75
Mean $\pm$ SD	0.12 $\pm$ 0.06	13.25 $\pm$ 2.14

Equation for pulmonary rib cage volume-esophageal pressure ( $V_{rc,p}$ - $P_{es}$ ) relation is as follows:  $V_{rc,p} = a \cdot P_{es} + b$ .

the diaphragm, and the abdominal muscles during quiet breathing and at the different levels of exercise in each subject (means  $\pm$  SE of all subjects). In contrast to quiet breathing, the inspiratory rib cage muscles and abdominal muscles developed greater mean pressures than the diaphragm at all exercise levels.

Fold changes over 0%  $\dot{W}_{max}$  of the same pressures are shown in Fig. 8. Figure 9 shows maximum changes in  $P_{di}$  and  $P_{rcm}$  (inspiratory + expiratory) during the respiratory cycle. In Fig. 9,  $\Delta P_{di}$  is the difference between passive  $P_{di}$  at the beginning of inspiration and active  $P_{di}$  at end inspiration. Thus, during exercise,  $\Delta P_{di}$  was less than the active  $P_{di}$  in Fig. 7. At the onset of exercise, there is a sudden shift in the pattern of respiratory pressure development with strong recruitment of abdominal muscles, so that the pressures they develop are virtually equal to those developed by the rib cage muscles. In contrast,  $\Delta P_{di}$  decreased from rest to exercise and increased little as exercise workload increased.

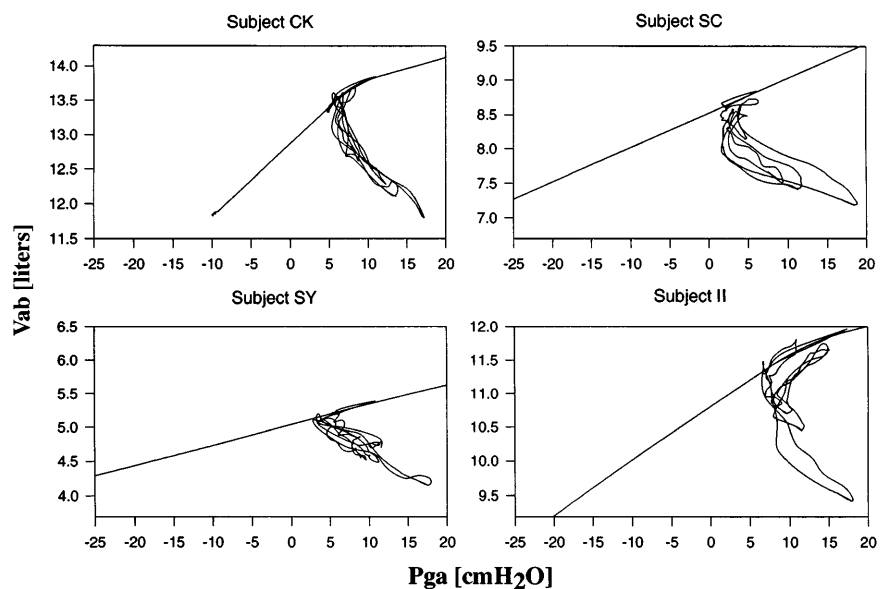
Figure 10 shows the time course of  $P_{rcm}$ ,  $P_{abm}$ , and  $P_{di}$  at different levels of exercise obtained as an average among the different subjects. Positive values of  $P_{rcm}$  are  $P_{rcm,i}$ , and negative values are  $P_{rcm,e}$ . The  $P_{di}$  curves contain active and passive components and show that the slope of the  $P_{di}$ -time curve during most of

inspiration in exercise was small, less than during quiet breathing and less than for  $P_{rcm}$  and  $P_{abm}$ .

In Fig. 11 the ratios of the pressures developed by the different muscle groups during quiet breathing to different levels of exercise are shown;  $P_{rcm,e}$ ,  $P_{di}$ , and  $P_{abm}$  have been referenced to  $P_{rcm,i}$ , because only the inspiratory rib cage muscles developed consistent pressures at rest and during exercise and monotonically increased from quiet breathing to the highest level of exercise. The data show that, in changing from rest to 0%  $\dot{W}_{max}$ , the relative pressure contributions of the four respiratory muscle groups changed abruptly. Thereafter, as exercise level increased, they did not change significantly, but their gains progressively increased.

The data in Figs. 7–10 indicate that the abdominal muscles produce the greatest pressures during exercise, increasing from 0 cmH<sub>2</sub>O during quiet breathing to ~40 cmH<sub>2</sub>O at 70%  $\dot{W}_{max}$ . The inspiratory rib cage muscles increased their pressure contribution from ~7 cmH<sub>2</sub>O during quiet breathing to ~30 cmH<sub>2</sub>O at 70%  $\dot{W}_{max}$ . Active  $P_{di}$  initially decreased from rest to 0%  $\dot{W}_{max}$ , and at 70%  $\dot{W}_{max}$  it only doubled on average compared with quiet breathing. The change in  $P_{di}$  from passive to active during exercise exceeded  $P_{di}$  during quiet breathing only at the highest workload. Expiratory rib cage muscles contributed a modest pressure, increasing from 0 to ~10 cmH<sub>2</sub>O from quiet breathing to 70%  $\dot{W}_{max}$ . Thus the changes in the pressure contributions of the various muscle groups were quite variable. However, when the data are normalized to the pressures during 0%  $\dot{W}_{max}$ , as shown in Fig. 8, the fold increases in pressure were similar for each muscle group. This is also shown in Fig. 11, which shows that the active pressures developed by the diaphragm, abdominal muscles, and expiratory rib cage muscles expressed as a fraction of the pressures developed by the inspiratory rib cage muscles changed

Fig. 6.  $V_{ab}$ - $P_{ga}$  loops during quiet breathing and increasing levels of exercise (0, 30, 50, and 70%  $\dot{W}_{max}$ ) and abdominal relaxation lines for 4 of 5 subjects. Fifth subject is not shown, because we were unable to obtain satisfactory relaxation curves.



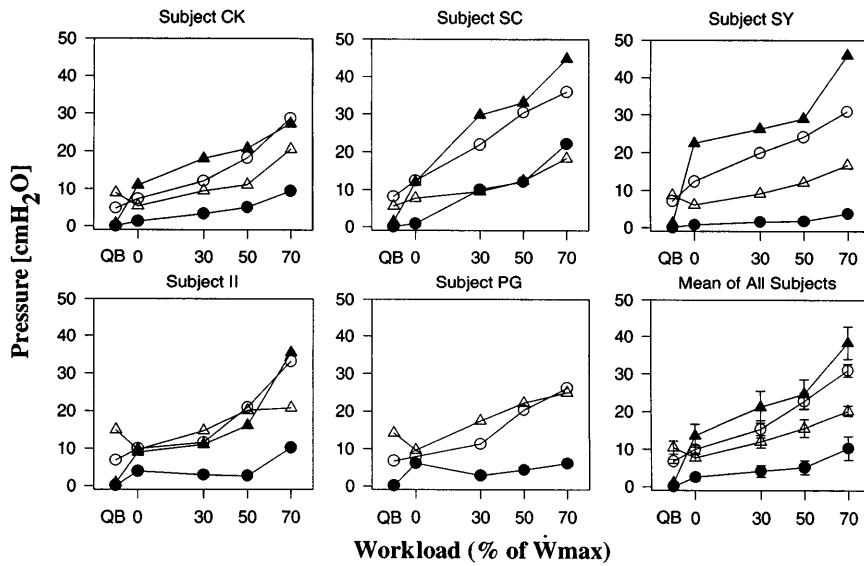


Fig. 7. Mean peak pressures developed by inspiratory rib cage muscles (○), expiratory rib cage muscles (●), diaphragm (△), and abdominal muscles (▲) during quiet breathing and different levels of exercise for each subject and mean values for all subjects.

from rest to 0%  $\dot{W}_{max}$  but thereafter remained constant as exercise increased.

**DISCUSSION**

*Physiological Significance of Chest Wall Volume Change*

The average decrease in end-expiratory  $V_{cw}$  of 0.98 liter that we measured during heavy exercise (Fig. 2) is generally in agreement with that reported in previous studies in which end-expiratory  $V_L$  decreased from 0.7 to >1.0 liter during heavy or maximal exercise (17, 19, 28). In addition, during heavy exercise, ~28% of  $V_T$  was accomplished below FRC and ~40% of the increase in  $V_T$  was attributable to the recruitment of expiratory reserve volume (Fig. 2). Although the reduction of end-expiratory  $V_L$  as an important contribution to  $V_T$  during exercise has been recognized for some time,

quantitative partitioning of this change into the contribution of the rib cage and abdomen has not been measured accurately. Earlier studies (15, 16, 27) showed a consistent reduction in end-expiratory  $V_{ab}$  during exercise; the change in end-expiratory rib cage volume ( $V_{rc}$ ) was less consistent. These studies estimated  $V_{cw}$  by magnetometry or respiratory inductive plethysmography. Such methods are subject to error, because they assume that the chest wall moves with only two degrees of freedom. Konno and Mead (21) showed that this was true over only limited degrees of rib cage and abdominal displacements. The present study avoids this problem by taking into account motion at many

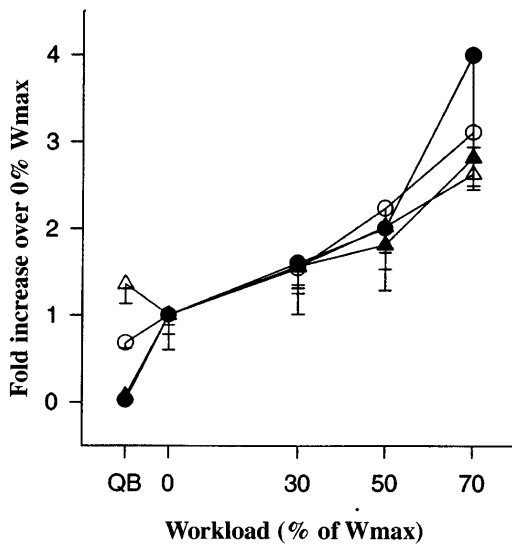


Fig. 8. Increase in pressures developed by inspiratory and expiratory rib cage muscles, diaphragm, and abdominal muscles for all subjects referred to 0%  $\dot{W}_{max}$ . Values are means  $\pm$  SE. Symbols as in Fig. 7.

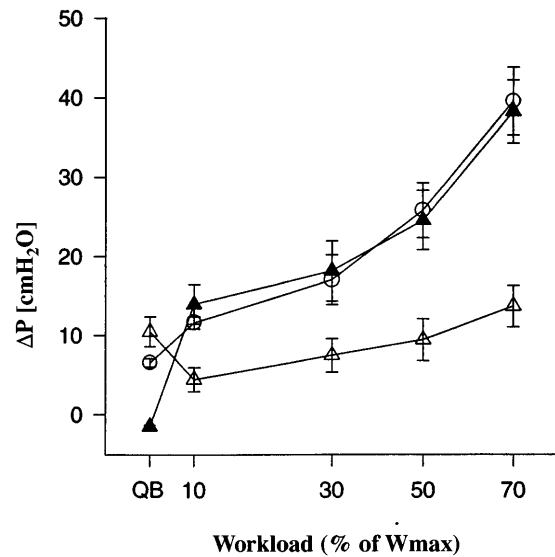


Fig. 9. Pressure changes ( $\Delta P$ ) in inspiratory + expiratory rib cage muscles and diaphragm from beginning to end inspiration and in abdominal muscles from end inspiration to end expiration during quiet breathing and at different levels of exercise for all subjects.  $\Delta P_{di}$  is difference between passive  $P_{di}$  at beginning of inspiration and active  $P_{di}$  at end inspiration. Values are means  $\pm$  SE. ○, Inspiratory + expiratory rib cage muscles; △, diaphragm; ▲, abdominal muscles.

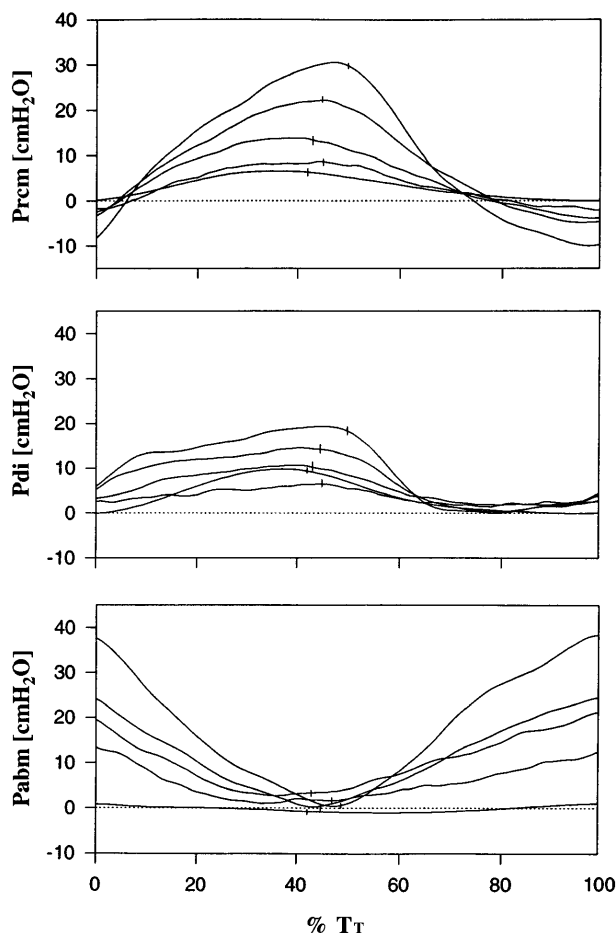


Fig. 10. Absolute mean Prcm, Pdi, and Pabm as a function of percent total respiratory cycle time (%Tr) obtained by normalizing time courses of rib cage, diaphragm, and abdominal muscle pressures of all subjects during quiet breathing and at all levels of exercise. Time courses of Prcm and Pabm were obtained by method described in Fig. 1 legend; Pdi was measured directly by Pga - Pes. Segments represent end-inspiratory zero-flow points.

points on the chest wall. This clearly demonstrates that the reduction in end-expiratory Vcw and, therefore, VL was almost entirely due to a decrease in end-expiratory Vab during exercise (Figs. 2 and 3A). End-expiratory Vrc,p and Vrc,a did not change significantly. Our recent study (29) showed little change in end-inspiratory abdominal diameter during exercise. The present results support this observation by demonstrating that end-inspiratory Vab was nearly constant, so the increase in end-inspiratory VL was almost entirely due to rib cage expansion (Figs. 3 and 4A). In other words, during exercise, the increase in rib cage VT resulted from recruiting only its inspiratory reserve volume, while the increase in abdominal VT largely resulted from recruiting only its expiratory reserve volume. Despite different recruitment patterns, the relative contributions to VT from RCp, RCa, and the abdomen remained nearly constant, although VT more than tripled during exercise. This arrangement has important physiological significance for the mechanics of breathing during exercise.

First, the behavior of the chest wall during exercise can be explained on the basis of the mechanical advantage of the inspiratory muscles. From residual volume (RV) to total lung capacity (TLC), the human diaphragm shortens by 30–35% during relaxation (4, 14) and presumably even more when contracted, reducing its ability to generate force and velocity of shortening. In addition to VL,  $L_{di}$  is also critically dependent on chest wall configuration. During an isovolume maneuver, for example, there is considerable change in  $L_{di}$  going from the belly-in to the belly-out configuration. Decreasing end-expiratory Vab at constant Vrc will increase  $L_{di}$ , whereas failure to increase end-inspiratory Vab will prevent excessive shortening. This tends to optimize diaphragm performance (4). On the other hand, the optimal length of the parasternal intercostals is shorter than its FRC length. Thus one may expect that the parasternal intercostals progressively approach their optimal length, improving their performance with increasing Vrc (9, 18). If Vrc decreased, the rib cage muscles would lengthen further from their optimal length, which would put them at a mechanical disadvantage. Therefore, our present results, which demonstrate a significant decrease in end-expiratory and a constant end-inspiratory Vab with a constant end-expiratory and increasing end-inspiratory Vrc during exercise, are consistent with optimization of the diaphragm by increasing its preinspiratory length and preventing excessive shortening during inspiration; similarly, inspiratory rib cage muscle performance is optimized by enhancing shortening during inspiration and preventing excessive preinspiratory lengthening.

Second, the different behavior of the rib cage and abdomen during exercise may also be explained by the

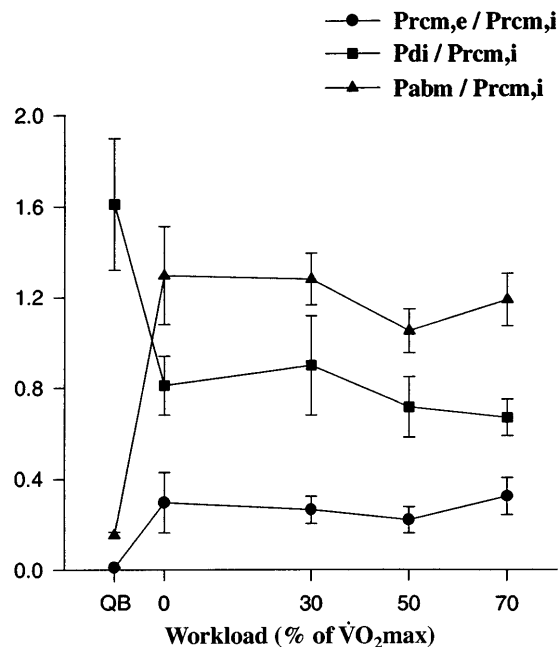


Fig. 11. Peak pressures of different respiratory muscles during quiet breathing plotted against different levels of exercise [maximal  $\dot{V}O_{2max}$ ] for all subjects. Values are means  $\pm$  SE. Prcm,e and Prcm,i, expiratory and inspiratory rib cage pressure, respectively.

mechanical characteristics of the rib cage and abdomen. Konno and Mead (22) showed that although rib cage compliance changes little with increasing volume, abdominal compliance markedly decreases as its volume increases. In addition, the inspiratory reserve volume is proportionately greater in the rib cage, and the expiratory reserve volume is proportionately greater in the abdominal compartments (12, 22). Therefore, during exercise with increasing demand for ventilation, decreasing end-expiratory  $V_L$  primarily by decreasing end-expiratory  $V_{ab}$  may be viewed as a means to utilize the most compliant compartments to minimize the elastic work of moving the chest wall. Whereas this would involve substantial distortion away from the minimal energy configuration that would increase work, it has been shown that the mechanical linkage between the rib cage and abdomen is small (10).

#### Diaphragm Length, Velocity of Shortening, and Power

$L_{di}$  is determined by  $V_L$  and chest wall configuration (14, 23). We have modeled  $\Delta V_{cw}$  as the sum of  $\Delta V_{rc,p}$ ,  $\Delta V_{rc,a}$ , and  $\Delta V_{ab}$  and measured the volume changes in these compartments by the ELITE system at rest, during quiet breathing, and at different levels of exercise, so we knew the chest wall configuration at any instant during breathing. This enables us to assess changes in  $L_{di}$  in our subjects.

The abdomen-diaphragm forms a single compartment, the peritoneal cavity, which contains the abdominal contents. It is essentially incompressible, so the sum of the volume under the diaphragm and the volume elsewhere in the peritoneal cavity is a constant. Therefore, any volume change in the contents of the diaphragm must be equal and opposite to the volume swept by the abdominal wall or  $\Delta V_{ab}$ . However, if the diaphragm changed shape as it shortened and displaced its contents into the abdominal wall, then  $L_{di}$  would be determined by two factors:  $\Delta V_{ab}$  and the changing surface-to-volume ratio of the diaphragm. Mead and Loring (23) showed that  $L_{di}$  was not uniquely determined by  $\Delta V_{ab}$  and that  $\Delta V_{rc,a}$  also played a significant role. If this is so,  $\Delta V_{rc,a}$  must reflect a change in the surface-to-volume ratio of the diaphragm. Inasmuch as a sphere is the shape with the smallest surface-to-volume ratio, this might occur by shortening of diaphragmatic fibers in the area of apposition, so that less of the diaphragmatic contents are contained in a cylinder-like structure and more in a dome-like structure. It can easily be shown that a change in shape from a cylinder to a sphere at constant volume and with equal radius of curvature decreases area by  $\sim 16.5\%$ . Gauthier et al. (14) showed that all diaphragmatic shortening occurred in the area of apposition, whereas the fibers in the dome increased in length. Thus a shape change from more cylindrical to more spherical probably occurs.

On the basis of the above considerations, we can now interpret exercise-induced changes in  $L_{di}$  according to our compartmental  $V_{cw}$  measurements. With increasing intensity of exercise, preinspiratory changes in  $L_{di}$  are uniquely determined by  $V_{ab}$ , since end-expiratory

$V_{cw}$  decreases solely because of a decrease in end-expiratory  $V_{ab}$  at constant end-expiratory  $V_{rc,a}$ . End-inspiratory changes in  $L_{di}$  are largely determined by end-inspiratory  $V_{rc,a}$ , since end-inspiratory  $V_{cw}$  increases because of an increase in end-inspiratory  $V_{rc}$  at a nearly constant end-inspiratory  $V_{ab}$ .  $V_{rc,p}$  has little direct effect on  $L_{di}$  because, except for a small slip of the costal diaphragm originating from the bottom of the sternum, the diaphragm is not attached to  $RC_p$ . Any effect of  $\Delta V_{rc,p}$  on  $L_{di}$  must be indirect through the mechanical linkage between  $RC_p$  and  $RC_a$  (30).

In addition, we found that, during resting breathing and at increasing levels of exercise,  $\Delta V_{rc,a}/\Delta V_{ab}$  during inspiration remained constant (Fig. 4). On the basis of the above analysis that changes in  $L_{di}$  are determined by  $\Delta V_{rc,a}$  and  $\Delta V_{ab}$ , we assume

$$\Delta L_{di} = \Delta L_{di(RC)} + \Delta L_{di(AB)}$$

$$\Delta L_{di(RC)} = k_1 \Delta V_{rc,a}$$

$$\Delta L_{di(AB)} = k_2 \Delta V_{ab}$$

where  $\Delta L_{di}$  is a diaphragmatic length change,  $\Delta L_{di(RC)}$  and  $\Delta L_{di(AB)}$  are fractions of diaphragmatic length change contributed by  $\Delta V_{rc,a}$  and  $\Delta V_{ab}$ , respectively, and  $k_1$  and  $k_2$  are constants. Then

$$\Delta L_{di} = k_1 \Delta V_{rc,a} + k_2 \Delta V_{ab}$$

Because  $\Delta V_{rc,a}/\Delta V_{ab}$  is also constant

$$\Delta V_{rc,a} = k_3 \Delta V_{ab}$$

where  $k_3$  is another constant. Substituting

$$\Delta L_{di} = (k_1 k_3 + k_2) \Delta V_{ab}$$

or

$$\Delta L_{di} = \text{constant} \Delta V_{ab} \quad (1)$$

During inspiration, although  $\Delta L_{di}$  is determined by  $\Delta V_{ab}$  and  $\Delta V_{rc,a}$ , it is proportional to  $\Delta V_{ab}$ , because  $\Delta V_{rc,a}/\Delta V_{ab}$  is constant. Thus our fortuitous finding of a constant  $\Delta V_{ab}/\Delta V_{rc,a}$  during exercise allows us to infer not only the length change but also the velocity of shortening of the diaphragm during exercise.

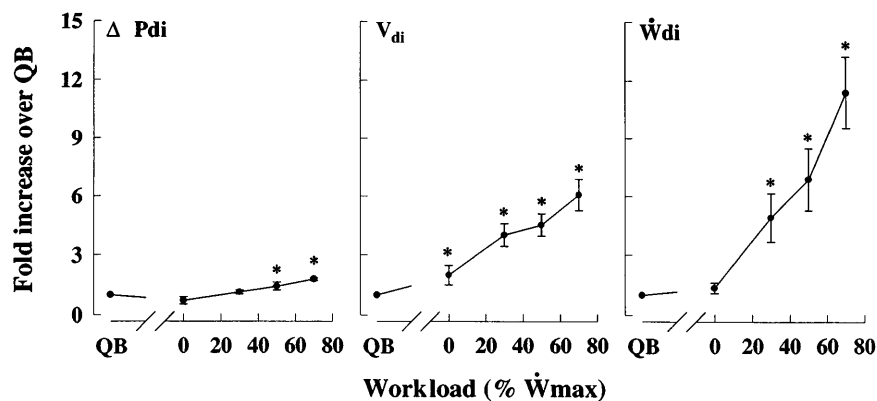
Dividing Eq. 1 by the inspiratory time ( $T_I$ ), we obtain

$$\Delta L_{di}/T_I = \text{constant} \cdot \Delta V_{ab}/T_I \quad (2)$$

The left-hand side of Eq. 2 is an expression of diaphragmatic mean velocity of shortening ( $V_{di}$ ), which is proportional to  $\Delta V_{ab}/T_I$ . Accordingly, the product of  $\Delta P_{di}$  and  $\Delta V_{ab}/T_I$  can be used as an index of diaphragmatic power output ( $\dot{W}_{di}$ ) during exercise. Although one cannot obtain absolute values of  $L_{di}$ ,  $V_{di}$ , and  $\dot{W}_{di}$ , inasmuch as the values of the constant in Eq. 2 are unknown, important information can be obtained with regard to how these variables change during quiet breathing and at different levels of exercise. In Fig. 12,  $\Delta P_{di}$ ,  $V_{di}$ , and  $\dot{W}_{di}$  thus calculated and normalized as a fraction of that during quiet breathing are plotted against workload. Our results suggest that, with increasing intensity of exercise,  $\dot{W}_{di}$  increased  $\sim 13$ -fold



Fig. 12. Increases in Pdi, diaphragmatic velocity of shortening ( $V_{di}$ ), and diaphragmatic power ( $\dot{W}_{di}$ ) from rest (quiet breathing) to 70%  $\dot{W}_{max}$ . Values are means  $\pm$  SE. \* $P < 0.05$  compared with QB.



largely due to a  $>6$ -fold increase in  $V_{di}$ , despite a less than doubling of  $\Delta P_{di}$  during breathing. In other words, the diaphragm during exercise behaves essentially as a flow generator rather than a pressure generator.

That the diaphragm largely works as a flow generator during exercise would be consistent with its *in vivo* shortening ability being greater than that of inspiratory rib cage muscles (4, 9, 14), but to act this way,  $\Delta P_{di}$  must be minimized. During exercise, abdominal muscle recruitment during expiration accounts for the reduction in FRC, whereas its gradual relaxation causes  $P_{ab}$  to fall throughout inspiration, in striking contrast to the rise in  $P_{ab}$  during quiet breathing (Fig. 6). The inspiratory fall in  $P_{ab}$  parallels the inspiratory fall in  $P_{pl}$ . Thus it is the gradual inspiratory abdominal muscle relaxation that minimizes  $\Delta P_{di}$ , unloading the diaphragm and making it able to generate high flows to meet ventilatory demands. We conclude that the diaphragm's main role during exercise is to generate flow, rather than pressure, and that its 13-fold increase in power from quiet breathing to 70%  $\dot{W}_{max}$  (Fig. 12) is due mainly to an increase in  $V_{di}$ .

If, however, the diaphragm primarily generates flow while only doubling  $P_{di}$ , the pressure required to displace the abdomen and rib cage must be produced by other muscles. Evidently, the abdominal muscles are used to displace the abdomen, and the rib cage muscles are used to displace the rib cage.

#### Velocity and Power of Rib Cage and Abdominal Muscles

From the pressure-volume curves of RCp and the abdomen in Figs. 5 and 6 and their time relationships, we obtained data for velocity of shortening and power for rib cage muscles from  $dV_{rc,p}/dt$  and  $\int P_{rcm} \cdot dV_{rc,p}/dt$  and for abdominal muscles from  $dV_{ab} \cdot dt$  and  $\int P_{abm} \cdot dV_{ab}/dt$  (Fig. 13). Figure 13, *top*, shows fold increases in power from 0%  $\dot{W}_{max}$ . The data for the diaphragm were calculated by using mean  $\Delta P_{di}$  between zero-flow points (*top trace*) or mean active  $P_{di}$  throughout inspiration. The power of the different muscles increased monotonically from 0 to 70%  $\dot{W}_{max}$ , with  $\dot{W}_{di}$  increasing 9- to 13-fold and inspiratory rib

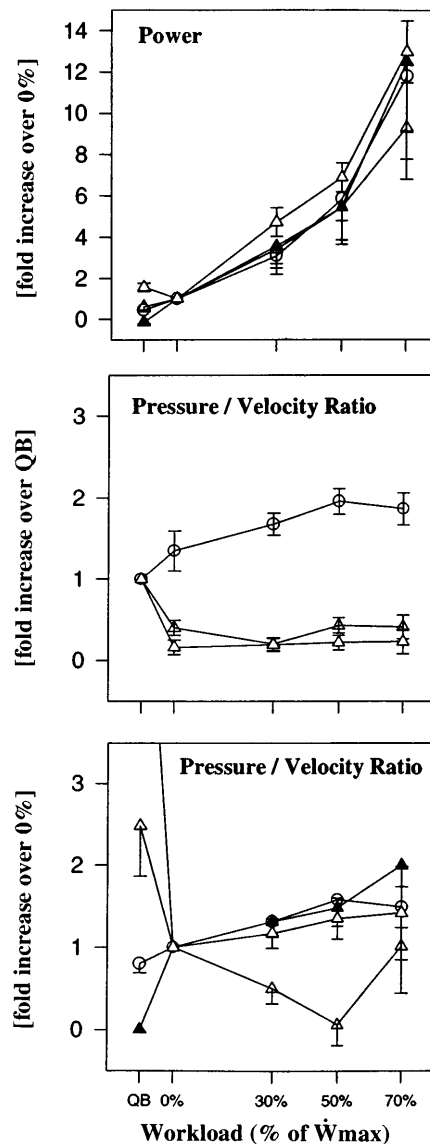


Fig. 13. *Top*: increase over 0%  $\dot{W}_{max}$  of different muscles.  $\Delta$ ,  $\dot{W}_{di}$ ;  $\circ$ , power of inspiratory rib cage muscles ( $\dot{W}_{rcm,i}$ );  $\blacktriangle$ , power of abdominal muscles ( $\dot{W}_{abm}$ ). *Middle*: increase over quiet breathing of mean pressure-to-velocity ratios of inspiratory rib cage muscles ( $\circ$ ) and diaphragm ( $\Delta$ ). *Bottom*: increase over 0%  $\dot{W}_{max}$  of mean pressure-to-velocity ratios of inspiratory rib cage muscles ( $\circ$ ), diaphragm ( $\Delta$ ), and abdominal muscles ( $\blacktriangle$ ).

cage muscle power ( $\dot{W}_{rcm,i}$ ) and abdominal muscle power ( $\dot{W}_{abm}$ ) increasing 12-fold.

Figure 13, *middle* and *bottom*, shows the pressure-to-velocity ratio of the different muscles to identify the degree to which the power developed by muscle groups was expressed as velocity of shortening or as force. Figure 13, *middle*, shows data for the diaphragm and inspiratory rib cage muscles. Whereas the pressure-to-velocity ratio of inspiratory rib cage muscles doubled with exercise, that of the diaphragm decreased to ~20% of its value over quiet breathing. Although most of  $\dot{W}_{di}$  is expressed as velocity of shortening during exercise, most of  $\dot{W}_{rcm,i}$  and  $\dot{W}_{abm}$  (data not shown) was expressed as force. Figure 13, *bottom*, shows pressure-to-velocity ratios normalized to 0%  $W_{max}$  for the muscle groups. These ratios remained almost independent of exercise workload, once exercise started. We will argue that a simple central control mechanism accounts for all these findings and minimizes rib cage distortion (20). Before doing so, various assumptions and possible sources of error need to be considered.

### Critique of Methods

In addition to the limitations and assumptions of the model of Ward et al. (30), which they discussed, we must account for the errors inherent in our estimates of the pressures developed by the different respiratory muscles. The estimation of  $P_{rcm}$  and  $P_{abm}$  is sensitive to the accuracy of the relaxation lines. It is conceivable that the elevated arm position we used during exercise might have inflated and stiffened the rib cage. We believe that this is unlikely, inasmuch as Konno and Mead (22) found that rib cage compliance was little affected by increasing volume, whereas abdominal compliance was markedly stiffened. In any event, strictly speaking, our results are applicable only to the exercise and its posture. We have assumed that the relaxation curve of the  $RC_p$  ( $P_{es}$  vs.  $V_{rc,p}$ ) was linear. This may not be true at  $V_L$  near TLC and RV. At large  $V_{rc,p}$ , linear extrapolation is an approximation that might lead to an underestimation of  $P_{rcm,i}$ . Similarly, at values of  $V_{rc,p}$  close to RV, linear extrapolation might lead to an underestimation of  $P_{rcm,e}$ , mainly for the highest level of exercise. We used the criteria of repeatability and zero  $P_{di}$  to validate the relaxation curves, but we obtained no data below FRC. This posed particu-

lar problems for the abdomen, inasmuch as virtually all the data of abdominal volume displacement were below FRC. The elastic behavior of the abdomen is, in fact, nonlinear (22) and is difficult to assess precisely, because it is difficult to perform reliable relaxation maneuvers below FRC. To partially circumvent this problem, we used quiet breathing inspiratory  $P_{ga}$  and  $V_{ab}$  values as the elastic behavior of the abdomen, because during quiet inspiration the action of the abdominal muscles is negligible (7).

We found a curvilinear relationship, to which we fitted a second-order polynomial. We linearly extrapolated these to high and low values of  $V_{ab}$ . The coefficients of the polynomial regression are given in Table 2. The linear extrapolation below FRC can lead to an overestimate of  $P_{abm}$  values, mainly at very low values of  $V_{ab}$ . We believe that the errors due to extrapolation of relaxation curves are not sufficient to affect our results qualitatively, although results from nonextrapolated curves might be different in detail. To the extent that the model represents reality,  $dV_{rc,p}/dt$  and  $dV_{ab}/dt$  should be reasonable indexes of the velocity of shortening of rib cage and abdominal muscles. As shown above, the velocity of diaphragmatic shortening is directly proportional to  $\Delta V_{ab}/T_1$ . Thus we can estimate average fold changes in diaphragmatic power or velocity of shortening but not absolute or instantaneous values.

The model provides only for a mechanical interaction between  $RC_p$  and  $RC_a$  when these two compartments are distorted from their relaxation configuration. In reality, axial strain of either compartment in the absence of distortion would produce stress on the other. This may be the reason that the dynamic  $V_{rc,a}$ - $P_{ga}$  relationships during exercise were frequently to the left of the relaxation line (data not shown), whereas during quiet breathing they were to the right (20).

### Dynamics and Control of Respiratory Muscles During Quiet Breathing and Exercise

Our analysis clearly shows that two completely different patterns of muscular recruitment occurred at rest and during exercise. In quiet breathing, we assume that abdominal muscles were phasically inactive, so that only the inspiratory muscles contracted, with the diaphragm generating more pressure than the inspiratory rib cage muscles; at the lowest level of exercise,

Table 2. Coefficients of abdominal relaxation lines

Subject	c, l/cmH <sub>2</sub> O	d, liters	e, l/cmH <sub>2</sub> O <sup>2</sup>	f, l/cmH <sub>2</sub> O	g, liters	h, l/cmH <sub>2</sub> O	i, liters	x <sub>1</sub> , cmH <sub>2</sub> O	x <sub>2</sub> , cmH <sub>2</sub> O
CK	0.106	12.87	-5.6e-3	0.163	12.72	0.032	13.49	5.04	11.64
SC	0.051	8.52	-1.8e-5	0.050	8.52	0.051	8.52	2.30	5.97
SY	0.031	5.04	-2.8e-4	0.034	5.03	0.028	5.06	5.99	11.17
II	0.079	10.81	-2.3e-3	0.111	10.70	0.029	11.42	6.82	17.56
Mean ± SD	0.067 ± 0.028	8.31 ± 2.90	-2.0e-3 ± 2.2e-3	0.089 ± 0.051	9.24 ± 2.85	0.037 ± 0.010	9.62 ± 3.17	5.04 ± 1.70	11.58 ± 4.11

Relaxation curve of abdomen was obtained from end-expiratory abdominal volume to end-inspiratory abdominal volume during quiet breathing by a 2nd-order polynomial regression of data of gastric pressure [ $P_{ga}$ , an index of abdominal pressure ( $P_{ab}$ )] and abdominal volume ( $V_{ab}$ ) and then extrapolated linearly for higher and lower values of  $V_{ab}$ , imposing continuity of 1st derivative.  $x_1$ , Mean value of  $P_{ga}$  at end expiration during quiet breathing;  $x_2$ , mean value of  $P_{ga}$  at end inspiration during quiet breathing. For  $P_{ga} < x_1$ , abdominal relaxation line is straight line  $V_{ab} = c \cdot P_{ga} + d$ ; for  $x_1 < P_{ga} < x_2$ , it is described by nonlinear equation  $V_{ab} = e \cdot P_{ga}^2 + f \cdot P_{ga} + g$ ; for  $P_{ga} > x_2$ , abdominal relaxation line is straight line  $V_{ab} = h \cdot P_{ga} + i$ .

however, the inspiratory rib cage muscles developed more pressure than the diaphragm (Figs. 7, 9, and 11). The abdominal muscles were significantly recruited even at the lowest level of exercise, with  $P_{abm}$  of greater magnitude than  $P_{rcm,i}$  (Fig. 11).  $\Delta P_{abm}$  was equal and opposite in magnitude to the sum of  $\Delta P_{rcm,i}$  and  $\Delta P_{rcm,e}$  (Figs. 9 and 10).

The relative values of the pressures developed by the different muscles changed abruptly from rest to 0%  $\dot{W}_{max}$  but thereafter remained constant (Fig. 11), and the fold increase over 0%  $\dot{W}_{max}$  with increasing exercise of  $P_{rcm,i}$ ,  $P_{rcm,e}$ ,  $P_{di}$ , and  $P_{abm}$  was similar (Fig. 8). The fold increases of  $W_{di}$ ,  $W_{rcm,i}$ , and  $W_{abm}$  over 0%  $\dot{W}_{max}$  were also similar (Fig. 13). The pressure-to-velocity ratios during exercise of inspiratory rib cage muscles, the diaphragm, and the abdomen changed little relative to 0%  $\dot{W}_{max}$  up to 70%  $\dot{W}_{max}$ , although for the diaphragm and inspiratory rib cage muscles they were strikingly different from rest (Fig. 13). Thus the behavior of the different muscle groups, once established, at 0%  $\dot{W}_{max}$  did not change throughout exercise, although it was very different from the behavior at rest. Clearly, there is an abrupt change in the control of the respiratory muscles at the onset of exercise, which thereafter remains constant but with increasing gain as exercise increases.

This suggests that the motor command from the brain stem respiratory centers increases similarly for all respiratory muscle groups as exercise level increases. However, whether that command is transduced into force or velocity of shortening depends on the load against which the muscles act once they are activated. Because of the gradual relaxation of abdominal muscles and the resulting fall in  $P_{ab}$  throughout inspiration (Figs. 6 and 10) in parallel with the fall in  $P_{pl}$ , the load on the diaphragm is minimized, allowing most of the diaphragmatic command to be transduced to velocity of shortening (Figs. 12 and 13). The abdominal muscles must therefore drive the abdomen, and they are responsible for all the decrease in end-expiratory lung volume. Because of their attachments at the costal margin, they exert a deflationary action on  $RCa$  during expiration, counteracting the effect of the increase in  $P_{ab}$ , whereas during inspiration their relaxation allows  $RCa$  to expand. Because of the load they must displace, their command is primarily converted to force. Similarly, the drive to rib cage muscles is also transduced primarily to force, inasmuch as they must develop the pressures required to overcome the load posed by the rib cage to increase end-inspiratory lung volume.

#### *How the Diaphragm Acts as a Flow Generator*

An ideal flow-generating muscle would contract isotonically, which for the diaphragm would minimize  $\Delta P_{di}$  during inspiration. Figures 9 and 10 show that this condition was largely met during exercise. At all levels of exercise,  $dP_{di}/dt$  was small during most of inspiration, less than during quiet breathing, and less than  $dP/dt$  of rib cage and abdominal muscles.

The low value of  $dP_{di}/dt$  was achieved by the action of the abdominal muscles. By displacing the abdomen inward during expiration, the diaphragm was stretched, so that at the onset of inspiration at all levels of exercise there was a passive  $P_{di}$  that increased as exercise level increased (Fig. 10). During inspiration the passive  $P_{di}$  was replaced by an active  $P_{di}$ . Yet  $P_{di}$  changed little, despite large falls in  $P_{pl}$  because of the gradual relaxation of abdominal muscles during inspiration. This action of abdominal muscles in lowering  $P_{ab}$  throughout inspiration and creating a passive  $P_{di}$  at the onset of inspiration would appear to be essential in allowing the conversion of the diaphragm's central drive to flow. This is presumably the reason why the dynamic  $V_{ab}$ - $P_{ga}$  curves, in contrast to  $V_{rc,p}$ - $P_{es}$  curves, are lines rather than loops (Figs. 1 and 6). If the abdominal muscles were to relax at the onset of inspiration, there would be an immediate fall in  $P_{ab}$  and the  $V_{ab}$ - $P_{ga}$  relationship would return to its relaxation curve. Subsequently,  $P_{ab}$  would have to increase while  $P_{pl}$  decreased during most of diaphragmatic contraction; as a result, the diaphragm would generate more pressure and less velocity for any given level of diaphragmatic activation.

#### *Minimization of Rib Cage Distortion and Transdiaphragmatic Pressure*

In addition to minimizing  $dP_{di}/dt$ , we believe that we have identified another important consideration in respiratory muscle control during exercise: the minimization of rib cage distortion. This must be done to maximize rib cage compliance, which during the distortion produced by an isolated diaphragmatic contraction is only 10% of its undistorted value (8, 20). How does the control system meet this constraint? The answer is astonishingly simple.

The zero rib cage distortion condition is met when there is no difference in the pressures acting on  $RCa$  and  $RCa$  (8, 20), i.e.

$$P_{rc,p} = P_{rc,a}$$

where  $P_{rc,a}$  is the elastic recoil pressure of  $RCa$ . The model described previously (20) indicates that, in the absence of distortion, there is no restoring force, so under equilibrium conditions the elastic recoil of  $RCp$  balances the combined effects of  $P_{pl}$  and  $P_{rcm}$

$$P_{rc,p} = P_{pl} + P_{rcm} \quad (3)$$

From consideration of the model and as shown by Eq. 5 in Ref. 20, we can write an equivalent expression for  $P_{rc,a}$

$$P_{rc,a} = xP_{di} + P_{ab} - yP_{abm} \quad (4)$$

where  $xP_{di}$  is the insertional component of  $P_{di}$  and  $0 \leq x \leq 1$ ;  $yP_{abm}$  is the insertional component of the abdominal muscles, where  $0 \leq y \leq 1$ , or that fraction of  $P_{abm}$  that acts directly on  $RCa$  to deflate it.

According to Eq. 4, the pressures acting on  $RCa$  are the insertional components of the diaphragm and abdominal muscles and  $P_{ab}$ , acting in the area of apposi-

tion. The actions of the diaphragm and Pab are inspiratory, whereas those of the abdominal muscles are expiratory (11, 24).

The pressure balance between RCp and RCa necessary for zero distortion is obtained by equating Eqs. 3 and 4

$$\begin{aligned} P_{pl} + P_{rcm} &= xP_{di} + P_{ab} - yP_{abm} \\ P_{rcm} &= (x + 1)P_{di} - yP_{abm} \end{aligned} \quad (5)$$

Therefore, an important part of the control strategy necessary for the respiratory muscles to avoid distortion is to maintain a fixed ratio between the pressures developed by the different muscle groups at any instant. Figure 11 shows that this was achieved. This helps maintain an equality between the pressures on RCa and RCp, preventing distortion (20). Distortion would arise from a difference in pressure, whichever muscle group generated it.

If we add to Eq. 5 the additional constraint that  $\Delta P_{di} \rightarrow 0$  and express it in terms of variations

$$\begin{aligned} \Delta P_{rcm} &= (x + 1)\Delta P_{di} - y\Delta P_{abm} \\ \Delta P_{rcm} &= -y\Delta P_{abm} \end{aligned} \quad (6)$$

Equation 6 states that to minimize Pdi and rib cage distortion all that is necessary is for the pressures developed by the rib cage muscles to be directly proportional to the pressures developed by the abdominal muscles and  $180^\circ$  out of phase. We therefore plotted  $\Delta P_{rcm}$  (inspiratory + expiratory) against  $\Delta P_{abm}$ . The results are shown in Fig. 14, and the slopes, intercepts, and  $r^2$  values of the regression line are given in Table 3. Figure 14 shows that the combined pressure swings of inspiratory and expiratory rib cage muscles were, on average, virtually identical to the average produced by the abdominal muscles. The relationship between the two are quasi-linear, with a slope of  $-1$ , and independent of exercise level.  $\Delta P_{rcm}$  led  $\Delta P_{abm}$  by only slightly  $>180^\circ$ . This remarkable finding is unlikely to be a coincidence. Indeed, we now show that the gradual relaxation of abdominal muscles is crucial in minimizing rib cage distortion and  $\Delta P_{di}$ .

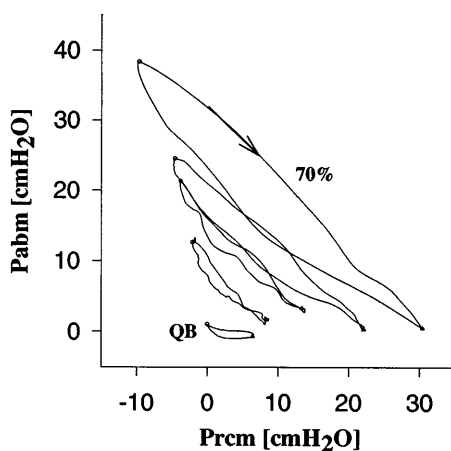


Fig. 14. Magnitude and phase of Prcm vs. Pabm during quiet breathing and at different levels of exercise.

Table 3. Slopes, intercepts, and  $r^2$  values of regression lines of Pabm-Prcm loops

	$m, \text{cmH}_2\text{O}$	$n$	$r^2$
QB	-0.17	0.30	0.34
0% $\dot{W}_{\text{max}}$	-1.01	8.83	0.91
30% $\dot{W}_{\text{max}}$	-1.03	15.21	0.94
50% $\dot{W}_{\text{max}}$	-0.86	18.31	0.92
70% $\dot{W}_{\text{max}}$	-0.90	26.59	0.91

$P_{abm} = m \cdot P_{rcm} + n$ , where Pabm and Prcm represent abdominal and rib cage muscle pressure, respectively (see Fig. 10). QB, quiet breathing;  $\dot{W}_{\text{max}}$ , maximal workload.

### Role of Abdominal Muscles in Exercise

Equation 6 describes Fig. 14 for all levels of exercise. It states that as Prcm increases during exercise, inflating RCp, Pabm decreases, allowing RCa to inflate. Because the data in Fig. 14 suggest that  $y = 1$ , Eq. 6 predicts that when  $\Delta P_{di} = 0$ , all the pressure developed by abdominal muscles must act on RCa.

Figure 10 shows that  $\Delta P_{di}$  was not actually zero but increased two- to threefold over its value at the onset of inspiration. Therefore, because the increase in Pdi has an inflationary action on RCa, the effect of abdominal muscle relaxation must be less. Because the transversus abdominis muscle has little or no effect on the rib cage (11), it is physiologically unlikely that the insertional component of Pabm is equal to Pabm and that  $y = 1$ . Apparently, there must be a compromise between the conflicting constraints that  $dP_{di}/dt = 0$  and that  $y < 1$ . The compromise is to allow  $dP_{di}/dt$  to increase to the point where it just compensates for  $y < 1$ .

To maintain the diaphragm as a flow-generating muscle while minimizing rib cage distortions [which were not zero (20)], a two- to threefold rise in Pdi occurred during inspiration, giving values for  $\Delta P_{di}/T_i$  in Figs. 9 and 10. At 30, 50, and 70%  $\dot{W}_{\text{max}}$  (Fig. 10),  $dP_{di}/dT_T$  (where  $T_T$  is respiratory cycle duration) was considerably larger early in inspiration, when flow rates were smaller. Thereafter  $dP_{di}/dT_T$  decreased, so that, from 0.2 to 1.0  $T_i$ ,  $dP_{di}/dT_T$  was nearly independent of exercise workload.

These considerations allot a triple role to the abdominal muscles during exercise: 1) their contraction during expiration accounts for all the decrease in end-expiratory volume, 2) their gradual relaxation during inspiration allows RCa to expand synchronously with RCp and minimizes the difference in pressure acting on the two rib cage compartments, and 3) the resulting fall in Pab throughout inspiration permits the diaphragm to act as a flow generator.

### Estimation of $x$ and $y$

Estimates of  $y$  can be obtained from the data. From Eq. 4

$$P_{rc,a} = xP_{di} + P_{ab} - yP_{abm}$$

If at end expiration we assume that  $xP_{di} \rightarrow 0$  (from Fig. 8 we see that passive Pdi at end expiration was 2.5–6.0  $\text{cmH}_2\text{O}$ , depending on exercise level, a value much



smaller than  $P_{abm}$  and calculated  $yP_{abm}$ ),  $yP_{abm}$  can be measured as  $P_{ab} - P_{rc,a}$  at end expiration. These values can be expressed as a fraction of  $P_{abm}$  to obtain  $y$ . As reported in Table 4, the insertional component of the abdominal muscle was 21–43% of  $P_{abm}$  (mean 30.5%). This is presumably an independent variable.

Estimates of  $x$  during exercise can also be obtained from the data. From Eq. 5, if it is assumed that at end inspiration  $P_{abm} \rightarrow 0$  (Fig. 8),  $x + 1$  can be computed as  $P_{rcm}/P_{di}$  at end inspiration. The results shown in Table 4 suggest that the diaphragmatic insertional component is  $\sim 40\%$   $P_{di}$ .

An alternative method to estimate  $x$  and  $y$  values is to compute the multiple linear regression among  $P_{rcm}$ ,  $P_{di}$ , and  $P_{abm}$  data, described by Eq. 5. Table 4 reports the results of the multiple regressions between  $P_{di}$  and  $P_{abm}$  values (independent variables) and  $P_{rcm}$  values (dependent variable) at all levels of exercise (0–70%  $W_{max}$ ) on the averaged data. The squared regression coefficient ( $r^2 = 0.93$ ) indicates that the fitting between the experimental data and the model was good. The intercept of the regression plane ( $k$ ) should ideally equal 0; in two subjects ( $SC$  and  $SY$ ) it has been estimated to be relatively high (10  $cmH_2O$ ), whereas in the other two subjects and in the averaged data it was low (0–3.5  $cmH_2O$ ). The constant  $k$  can be used to assess the accuracy of the estimation of  $P_{abm}$ ; in fact, the positive intercept  $k$  tends to counterbalance an overestimate of the negative term  $yP_{abm}$ : the higher the value of  $k$ , the higher the overestimation of  $P_{abm}$ . This is confirmed by the estimated abdominal relaxation lines of  $SC$  and  $SY$ , which are very similar to a straight line (Table 2) and tend to overestimate  $P_{abm}$ , mainly at the lowest abdominal volumes. The estimated values of  $x$ , the fraction of the total  $P_{di}$  that comprised inspiratory  $P_{di}$  (mean  $0.23 \pm 0.05$ ), are essentially in agreement with those reported by Ward et al. (30), even if our measurements are more accurate.

### Conclusions

We conclude that a simple control mechanism in which  $\Delta P_{rcm} = -\Delta P_{abm}$  accomplishes two remarkable feats simultaneously. It minimizes rib cage distortions and  $\Delta P_{di}$ . Given the constraint that  $y < 1$ ,  $\Delta P_{di}$  must rise to minimize distortions, but even at the highest levels of exercise that we studied it was not greater

Table 4. Insertional components of diaphragm and abdominal muscles estimated by a linear multiple regression of  $P_{rcm}$ ,  $P_{di}$ , and  $P_{abm}$  data and at end inspiration and end expiration

	Multiple Regression	Zero-Flow Points
$x$	$0.27 \pm 0.02$	$0.41 \pm 0.18$
$y$	$0.38 \pm 0.01$	$0.31 \pm 0.08$
$r^2$	0.93	
$k$	$2.40 \pm 0.30$	

Values are means  $\pm$  SE. See Eq. 5.  $r^2$  and  $k$ , Squared regression coefficient and intercept of multiple linear regression, respectively;  $x$  and  $y$ , insertional components of diaphragm and abdominal muscles, respectively;  $P_{di}$ , transdiaphragmatic pressure.

than during quiet breathing. This small increase in  $P_{di}$  allowed some rib cage distortions, but they remained small.

This analysis assigns two previously unrecognized roles to the abdominal muscles during exercise: they allow the diaphragm to contract quasi-isotonically, and they prevent rib cage distortion. The former role is played by allowing  $P_{ab}$  to decrease throughout inspiration, in parallel with  $P_{pl}$ , so that  $\Delta P_{di}$  is minimized. The latter role we ascribe to the deflationary action of abdominal muscles on  $RCa$ . End-expiratory  $V_{rc,a}$  changed little during exercise, yet end-expiratory  $P_{ab}$  and  $P_{di}$  increased substantially (Figs. 6 and 10). According to the model in Ref. 20, if there were no rib cage deflationary action of abdominal muscles, at end expiration  $RCa$  would be greatly expanded, whereas  $RCp$  would be contracted; distortions would be large. During inspiration the decline in  $P_{ab}$  of  $\sim 13$   $cmH_2O$  at 70%  $W_{max}$  with only a small increase in  $P_{di}$  would cause  $RCa$  to paradoxically deflate while  $RCp$  expanded. We suggest that the gradual relaxation of abdominal muscles during inspiration allowed  $RCa$  to expand and  $P_{di}$  to decrease. Indeed, according to the model, this is the only way  $RCa$  could have expanded. During expiration the strong abdominal muscle contraction counterbalanced the inflating action of  $P_{ab}$  and passive  $P_{di}$  on  $RCa$ , causing it to deflate along with  $RCp$ .

The model, however, ignores axial interactions between  $RCp$  and  $RCa$  in the absence of distortion and a direct action of inspiratory rib cage muscles on  $RCa$ . The fact that during exercise the inspiratory  $V_{rc,a}$ - $P_{ab}$  relationships were to the left of the relaxation line (data not shown) suggests axial stress from  $RCp$  or a direct action of inspiratory rib cage muscles on  $RCa$ . Furthermore, we have ignored any action of expiratory rib cage muscles on  $RCa$ .  $P_{rcm,e}$  on  $RCp$  were relatively small. These would include pressures developed by the triangularis sterni, which acts directly only on  $RCp$  and is an important rib cage expiratory muscle. Thus, although we believe that axial stresses from  $RCp$  and inspiratory and expiratory rib cage muscles may act directly on  $RCa$ , particularly at high exercise workloads, we also believe that the direct action of abdominal muscles on  $RCa$  counterbalances the effect of the increase in  $P_{ab}$  and passive  $P_{di}$  on  $RCa$  during expiration. Because this effect of abdominal muscles should be a direct function of the tension within abdominal muscles regardless of whether it is active or passive, the reason the  $V_{rc,a}$ - $P_{ab}$  relationship is to the right of the relaxation line during quiet breathing is presumably due to passive stretching of the abdominal muscles during inspiration (20).

We further conclude that the central drive to the various respiratory muscle groups changes during the transition from quiet breathing to exercise. The drive is  $180^\circ$  out of phase between rib cage and abdominal muscles and increases proportionately to all muscle groups as exercise workload increases, but whether the drive is translated into velocity of shortening or force depends on the load against which the muscles act. Because of abdominal muscle action, the load on the diaphragm is small, and most of the drive is converted

to shortening velocity. In contrast, the abdominal and rib cage muscles act primarily as force generators and develop the pressures required to displace the rib cage and abdomen.

This work was supported by the Medical Research Council of Canada, Respiratory Health Network of Centres of Excellence, Montréal Chest Institute, Allen and Hanburys Thoracic Society of Australia and New Zealand Fellowship, J. T. Costello Memorial Research Fund, and Fondazione Pro Juventute, Italy, Telethon Italy.

Address for reprint requests: P. T. Macklem, Montréal Chest Institute, 3650 St. Urbain, Montreal, Quebec, Canada H2X 2P4.

Received 24 July 1996; accepted in final form 17 April 1997.

## REFERENCES

1. **Agostoni, E., and E. D'Angelo.** Statics of the chest wall. In: *The Thorax*, edited by C. Roussos and P. T. Macklem. New York: Dekker, 1988, p. 259–295. (Lung Biol. Health Dis. Ser.)
2. **Agostoni, E., and P. Mognoni.** Deformation of the chest wall during breathing efforts. *J. Appl. Physiol.* 21: 1827–1832, 1966.
3. **Agostoni, E., and H. Rahn.** Abdominal and thoracic pressures at different lung volumes. *J. Appl. Physiol.* 15: 1087–1092, 1966.
4. **Brown, N. M. T., A. S. Narinder, and D. F. Rochester.** Force-length relationship of the normal human diaphragm. *J. Appl. Physiol.* 53: 405–412, 1982.
5. **Cala, S. J., C. M. Kenyon, G. Ferrigno, P. Carnevali, A. Aliverti, A. Pedotti, P. T. Macklem, and D. F. Rochester.** Chest wall and lung volume estimation by optical reflectance motion analysis. *J. Appl. Physiol.* 81: 2680–2689, 1996.
6. **Campbell, E. J. M.** *The Respiratory Muscles and the Mechanics of Breathing*. Chicago, IL: Year Book, 1958.
7. **Campbell, E. J. M., and J. H. Green.** The behaviour of the abdominal muscles and intra-abdominal pressure during quiet breathing and increased pulmonary ventilation: a study in man. *J. Physiol. (Lond.)* 127: 423–426, 1955.
8. **Chihara, K., C. M. Kenyon, and P. T. Macklem.** Human rib cage distortability. *J. Appl. Physiol.* 81: 437–447, 1996.
9. **Decramer, M., and A. De Troyer.** Respiratory changes in intercostal length. *J. Appl. Physiol.* 57: 1254–1260, 1984.
10. **Deschamps, C., J. R. Rodarte, and T. A. Wilson.** Coupling between rib cage and abdominal compartments of the relaxed chest wall. *J. Appl. Physiol.* 65: 2265–2269, 1988.
11. **De Troyer, A., M. Sampson, S. Sigrist, and S. Kelly.** How the abdominal muscles act on the rib cage. *J. Appl. Physiol.* 54: 465–469, 1983.
12. **Estenne, M., J.-C. Yernault, and A. De Troyer.** Rib cage and diaphragm-abdomen compliance in humans: effects of age and posture. *J. Appl. Physiol.* 59: 1842–1848, 1985.
13. **Farkas, G. A., M. Decramer, D. F. Rochester, and A. De Troyer.** Contractile properties of intercostal muscle and their functional significance. *J. Appl. Physiol.* 59: 528–535, 1985.
14. **Gauthier, A. P., S. Verbanck, M. Estenne, C. Segerbarth, P. T. Macklem, and M. Paiva.** Three-dimensional reconstruction of the in vivo human diaphragm shape at different lung volumes. *J. Appl. Physiol.* 76: 495–506, 1994.
15. **Grimby, A., J. Bunn, and J. Mead.** Relative contribution of rib cage and abdomen to ventilation during exercise. *J. Appl. Physiol.* 24: 159–166, 1968.
16. **Grimby, G., M. D. Goldman, and J. Mead.** Respiratory muscle action inferred from rib cage and abdominal V-P partitioning. *J. Appl. Physiol.* 41: 739–751, 1976.
17. **Henke, K. A., M. Sharratt, D. Pegelow, and J. A. Dempsey.** Regulation of end-expiratory lung volume during exercise. *J. Appl. Physiol.* 64: 135–146, 1988.
18. **Jiang, T. X., K. Deschepper, M. Demedts, and M. Decramer.** Effects of acute hyperinflation on the mechanical effectiveness of the parasternal intercostals. *Am. Rev. Respir. Dis.* 139: 522–528, 1989.
19. **Johnson, B. D., K. C. Seow, D. G. Pegelow, and J. A. Dempsey.** Adaptation of the inert gas FRC technique for use in heavy exercise. *J. Appl. Physiol.* 68: 802–809, 1990.
20. **Kenyon, C. M., S. J. Cala, S. Yan, A. Aliverti, G. Scano, R. Duranti, A. Pedotti, and P. T. Macklem.** Rib cage mechanics during quiet breathing and exercise in humans. *J. Appl. Physiol.* 83: 1242–1255, 1997.
21. **Konno, K., and J. Mead.** Measurement of the separate volume changes of rib cage and abdomen during breathing. *J. Appl. Physiol.* 22: 407–422, 1967.
22. **Konno, K., and J. Mead.** Static volume-pressure characteristics of the rib cage and the abdomen. *J. Appl. Physiol.* 24: 407–422, 1968.
23. **Mead, J., and S. H. Loring.** Analysis of volume displacement and length changes of the diaphragm during breathing. *J. Appl. Physiol.* 53: 750–755, 1982.
24. **Mier, A., C. Brophy, M. Estenne, J. Moxham, M. Green, and A. De Troyer.** Action of abdominal muscles on rib cage in humans. *J. Appl. Physiol.* 58: 1438–1443, 1985.
25. **Rahn, H., A. B. Otis, L. E. Chadwick, and W. O. Fenn.** The pressure-volume diagram of the thorax and lung. *Am. J. Physiol.* 146: 161–178, 1946.
26. **Rohrer, F.** Physiologie der Atembewegung. In: *Handbuch der normalen und pathologischen Physiologie*, edited by A. T. J. Bethe, G. von Bergmann, G. Emboden, and A. Ellinger. Berlin: Springer, 1925, p. 70–127.
27. **Sackner, J. D., A. J. Nixon, B. Davis, N. Atkins, and M. A. Sackner.** Effects of breathing through external dead space on ventilation at rest and during exercise. II. *Am. Rev. Respir. Dis.* 122: 933–940, 1980.
28. **Sharratt, M. T., K. A. Henke, E. A. Aaron, D. F. Pagelow, and J. A. Dempsey.** Exercise induced changes in functional residual capacity. *Respir. Physiol.* 70: 313–326, 1987.
29. **Sliwinski, P., S. Yan, A. P. Gauthier, and P. T. Macklem.** Influence of global inspiratory muscle fatigue on subsequent respiratory muscle activity during exercise. *J. Appl. Physiol.* 80: 1270–1278, 1996.
30. **Ward, M. E., J. W. Ward, and P. T. Macklem.** Analysis of human chest wall motion using a two-compartment rib cage model. *J. Appl. Physiol.* 72: 1338–1347, 1992.